The Force Field of Porphycene: A Theoretical and Experimental Approach

Karsten Malsch and Georg Hohlneicher*

Institut fuer Physikalische Chemie, Universitaet zu Koeln, Luxemburgerstr. 116, 50939 Koeln, Germany

Received: April 15, 1997; In Final Form: August 27, 1997[⊗]

The contribution deals with the theoretical and experimental examination of the force field of porphycene ([18]porphyrin-(2.0.2.0))—a structural isomer of porphyrin. Special care was taken for a possible tautomerism of the hydrogen atoms in the cavity of the molecule. We report IR, Raman, UV, as well as site-selective fluorescence and fluorescence excitation spectra. Most spectra were measured under matrix isolation conditions. Quantum chemical calculations based on density functional theory methods were used to derive force fields and IR intensities for the most probable tautomeric forms.

1. Introduction

Porphycene **1** ([18]porphyrin-(2.0.2.0)), synthesized in 1986 by Vogel and co-workers[1] was the first in a series of structural isomeres of porphyrin **2** ([18]porphyrin-(1.1.1.1)), frequently called pigment of life.[2] Together with corrphycene ([18]-porphyrin-(2.1.0.1))[3] and hemiporphycene ([18]porphyrin-(2.1.1.0)),[4,5] **1** led to a further diversification among the so-called porphyrinoids (see Chart 1).[6]

Similar to porphyrin, porphycene generated widespread theoretical and experimental interest. The possibility to compare two systems that differ only slightly and to thereby achieve a better understanding of porphyrin itself led to a considerable large number of new investigations on both systems.[7−31]

One question frequently raised in connection with porphyrinoids concerns the symmetry of the system and the amount of π-electron delocalization. Any kind of double-bond localization along the macrocyclic ring reduces the symmetry of porphyrin from D_{2h} to C_{2v} and makes the highly symmetric D_{2h} form a transition structure between two equivalent localized forms. A serious discussion of such a possibility[7] arose from the results of theoretical calculations: all restricted Hartree−Fock (RHF) calculations, whether semiempirical or ab initio and independent of basis set size, predict localized structures with C_{2v} symmetry to be more stable than the D_{2h} structure. In the meantime, Almloef et al.[8] demonstrated that this prediction is simply due to the neglect of correlation effects in RHF calculations. Since then it has been shown by several groups that almost every type of calculation that includes electron correlation to some extent (UHF,[9] MP2 and DFT,[8,10] CASSCF/CASPT2[11]) yields the D_{2h} structure. (It has to be mentioned that no geometry optimization was performed in ref 11 but that the results of the CASSCF/CASPT2 calculations strongly favored the D_{2h} structure.) A similar result was found for porphycene.[12−14] In these investigations density functional theory (DFT)-based methods turned out to be very efficient because of low cost in computer time.

Another question widely discussed in connection with porphyrin is the tautomerism of the two inner protons of the free base. The possible existence of an equilibrium between trans and cis forms has been examined extensively both theoretically[15,16] and experimentally, the latter primarily with ^{15}N-CPMAS NMR spectroscopy.[17−19] Compared to porphyrin the situation is further complicated in porphycene by the possible existence of two cis structures (see Chart 2).

CHART 1: [18]Porphyrin-(2.0.2.0), 1, and [18]Porphyrin-(1.1.1.1), 2

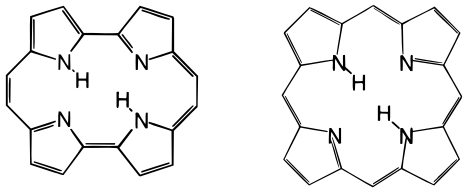

(1) (2)

CHART 2: Tautomerism in Porphycene

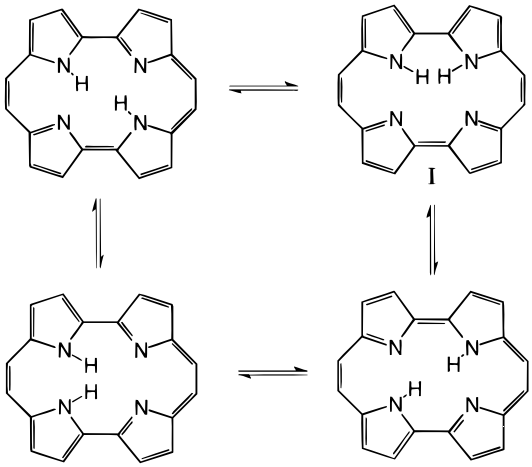

I II

On the basis of our quantum chemical calculations[13] we no longer consider structure II. This structure is predicted to be strongly destabilized compared to *trans*-porphycene and to the cis structure I. For the remainder of this paper, we refer to structure I simply as *cis*-porphycene. Calculations that go beyond the RHF level predict the trans form to be more stable by 6−10 kJ/mol, corresponding to an equlibrium contribution of the cis form of less than 5%.[13] The ^{15}N-CPMAS NMR investigations provided some indication for the existence of a tautomeric equilibrium,[17] and the estimated energy difference between the two components agrees with the calculated values.[32] However, the NMR investigations did not allow to determine which one is the more stable form: cis or trans. The same is true for UV−vis spectroscopy. The equilibrium partition of less than 5% cis proposed in ref 20 was based on the assumption

[⊗] Abstract published in *Advance ACS Abstracts,* October 15, 1997.

S1089-5639(97)01303-0 CCC: $14.00

of a highly localized structure of the cis form, an assumption that is probably incorrect (see ref 13 for further details).

In porphycene the tautomeric shift is accompanied by a change in the point group from C_{2h} to C_{2v} resulting in a loss of the inversion center. The exclusion principle is valid only for *trans*-porphycene, which means that vibrational spectroscopy should provide another possibility to derive information on the amount of *cis*-porphycene in a possible equilibrium. To follow this path we measured Raman and IR (KBr/CsI pellet and N_2 matrix) as well as site-selective laser-induced fluorescence and fluorescence excitation spectra (Ar matrix) of porphycene. Highly resolved spectra of this kind are so far only known for porphyrin[21−23] and its isotopomers.[24] These spectra were measured in rare-gas matrices, in a Shpolskii matrix,[25] and in supersonic jet spectroscopy.[26] Spectroscopic investigations on porphycene up to now have been restricted to low-temperature measurements in glasses,[20,27] which concentrated on the polarization of the different low-lying transitions.

In conjunction with the experimental measurements we also performed quantum chemical calculations to establish the force fields of *trans*- and *cis*-porphycene in harmonic approximation similar to those recently reported for porphyrin.[28−30] All theoretical results were obtained with DFT methods because of our prior experience with these methods in a variety of applications to porphyrinoids.[13,14,31]

2. Experimental Section

2.1. Sample Preparation. Samples of porphycene were used without further purification. The KBr/CsI pellets and the sample for the Raman spectrum were prepared using standard techniques. During matrix isolation porphycene was codeposited with nitrogen on a KBr window for the IR measurement and with argon on a sapphire window for the fluorescence measurements. The sample was kept at a temperature of 180 °C and a pressure of about 1×10^{-5} mbar during matrix preparation. The window was cooled to 27 K during this step. After completion of deposition, the window was cooled to 12 K and the measurements were carried out at that temperature. The dilution in the matrix was about 1:500.

2.2. Spectroscopic Equipment. The IR spectra of porphycene were measured with a Nicolet SX20 FTIR spectrometer. The Raman spectrum was measured with a Bruker FRA106 FT-Raman spectrometer. The UV spectrum of the matrix-isolated sample was recorded with a Beckmann UV−vis Spectrometer Acta MVI. The fluorescence and the fluorescence excitation spectra were measured using an apparatus described in ref 33. For excitation we used a Lambda Physics dye laser FL2002 pumped by a Lambda Physics excimer laser EMG101MSC. To determine the site structure of the porphycene−argon matrix a two-dimensional fluorescence and fluorescence excitation spectrum was recorded using a camera consisting of an array of 512 photodiodes (Spectroscopy Instruments IRY-512). The spectrum (Figure 1) reveals at least nine different sites. The best single-site spectra with a minimum of contamination from other sites are usually obtained when a low-energy site is used for the measurement of the fluorescence spectrum and a high-energy site for the determination of a fluorescence excitation spectrum. We chose the site with λ_{exc} = 626.12 nm (A) for the fluorescence and the site with λ_{det} = 630.89 nm (B) for the fluorescence excitation spectrum. In both cases a 1 m monochromator by Jobin-Yvon (THR 1000) was used as the dispersive element. The fluorescence signal was detected by a Hamamatsu R943-02 photomultiplier.

2.3. Calculations. All calculations were performed with the GAUSSIAN94[34] implementation of density functional theory.

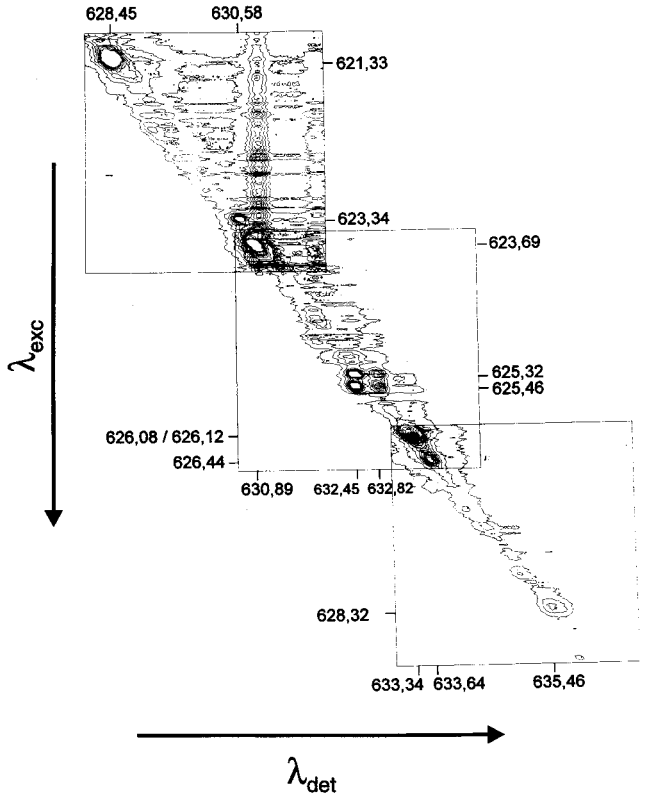

Figure 1. Two-dimensional fluorescence/fluorescence excitation spectrum of porphycene.

We applied the exchange potential (B)[35] proposed by Becke in combination with the correlation potential of Lee, Yang, and Parr (LYP).[36] The standard Gaussian basis sets 3-21G were used for all atoms except for the two hydrogen atoms in the cavity. These two atoms were modeled using a 6-31G** basis set. As has been shown before,[13,14] it is essential to supply the inner hydrogens with larger basis sets, especially with polarization functions, to model the hydrogen bonding in the cavity, i.e., to get realistic values for the lengths of the NH bonds. The calculations were restricted to C_{2h} and C_{2v} symmetry for *trans*-porphycene and *cis*-porphycene, respectively. The calculation of the minimum structure (reported elsewhere[13]) was followed by the determination of a harmonic force field and the calculation of the IR spectrum. The calculations were performed with the BLYP functional. Second derivatives were obtained numerically. The calculated frequencies were all real, indicating that the equilibrium geometries, obtained under symmetry restriction, are minima on the potential energy surface.

3. Experimental Results

3.1. Infrared Spectroscopy. The IR spectrum of porphycene measured under matrix isolation conditions at 12 K is shown in the lower panel of Figure 2. The upper panel shows the spectrum in KBr at room temperature. The wavenumbers and relative intensities of the observed bands are listed in Table 1. Table 1 also contains results from the measurement in a CsI pellet that extends down to 200 cm^{-1}. The signals at 2910 and 2850 cm^{-1} in the KBr spectrum have different relative intensities in differently prepared samples. Therefore, we attribute these bands to an impurity. The KBr and the matrix spectrum are very similar. The bands that appear at 559 and 583 cm^{-1} in the matrix spectrum do not belong to the sample. With our experimental setup they are always present in plain N_2 matrices. The only distinct differences between the N_2 matrix and the pellets is a band at 985 cm^{-1} and a group of

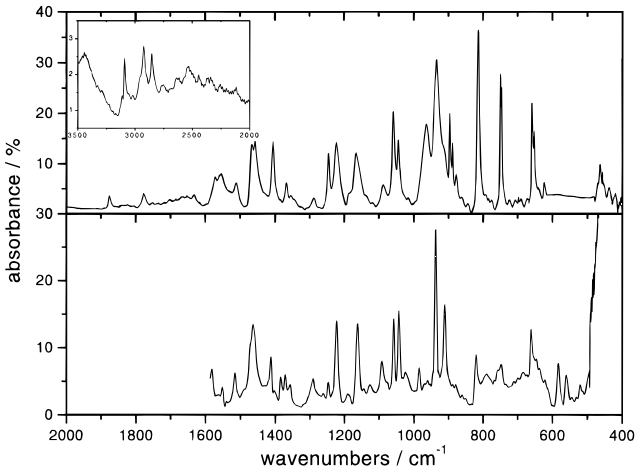

Figure 2. IR spectrum of porphycene in KBr (upper panel) and in N_2 matrix (lower panel).

TABLE 1: Energies and Relative Intensities in IR Spectra of Porphycene

KBr pellet		CsI pellet		N_2 matrix	
$\tilde{\nu}$/cm^{-1}	int	$\tilde{\nu}$/cm^{-1}	int	$\tilde{\nu}$/cm^{-1}	int
3091	8	3093	10		
1876	10	1877	22		
1777	10	1778	24		
1632	10	1631	16		
1571	24	1572	46	1581	25
1554	25	1556	48	1550	14
1511	19	1511	40	1515	21
				1473	39
1466	44	1467	71	1464	50
1457	46	1458	71		
1406	46	1406	72	1412	32
				1385	20
1367	21	1368	43	1370	21
1353	10	1354	26	1356	14
1287	10	1288	22	1291	20
1246	38	1246	66	1247	16
1222	46	1222	71	1222	54
1165	38	1166	69	1162	50
1088	19	1089	43	1090	29
1059	63	1059	89	1058	54
1044	46	1045	76	1042	57
				985	25
963	54	964	84		
935	100	936	100	937	100
910	40	912	45	911	61
896	63	897	90		
887	46	889	79		
878	21	878	54		
813	119	814	112	819	36
749	85	748	110	748	29
746	79				
		698	26		
659	65	659	107	662	46
652	46	653	94		
624	15	624	35		
				(583)	(6)
				(559)	(8)
464	31	464	66		
		384	30		
		314	43		
		233	20		
		223	15		
		217	6		

three bands around 890 cm^{-1} that appear only in the pellet spectra. There are no bands that appear to gain intensity in the KBr spectrum relative to the matrix spectrum. A similar result was found when the KBr pellet was measured at room temperature and at liquid nitrogen temperature. The spectrum

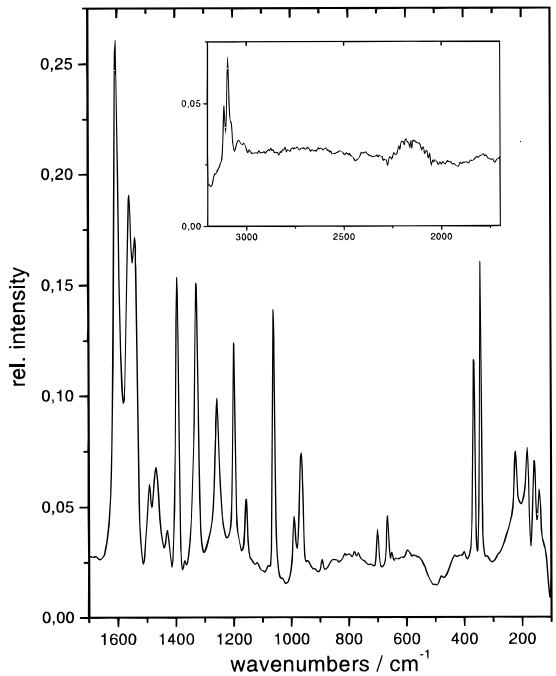

Figure 3. Raman spectrum of porphycene.

TABLE 2: Energies and Relative Intensities in the Raman Spectrum of Porphycene

$\tilde{\nu}$/cm^{-1}	int	$\tilde{\nu}$/cm^{-1}	int	$\tilde{\nu}$/cm^{-1}	int
3115	19	1327	58	650	8
3096	27	1258	39	597	12
3044	12	1198	48	479	6
1605	100	1158	22	400	12
1559	73	1115	10	367	46
1539	65	1061	54	344	65
1491	23	990	19	222	29
1468	27	965	29	182	30
1429	12	893	12	159	28
1395	58	701	17	141	23
1370	10	666	19		

did not show any temperature dependence. Irrespective of the form in which porphycene really exists, we do not observe indications for an equilibrium between the two nearly isoenergetic forms.

The spectrum is not very crowded with respect to the size of the molecule. The limited number of bands that appear in the IR spectrum seam to indicate a center of symmetry. Only half of the 108 normal modes (36 b_u and 18 a_u) are IR active under C_{2h} symmetry while the other half (37 a_g and 17 b_g) are Raman active. a_g and b_u are in-plane and a_u and b_g out-of-plane modes.

No indication of a NH stretching vibration is found in the usual range[37] around 3300 cm^{-1}. The only detectable bands that appear between 2500 and 3400 cm^{-1} are the CH bands around 3090 cm^{-1}. The absence of the NH stretching vibrations appearing at 3305 cm^{-1} in **2** has been attributed to the special geometry of the cavity in porphycene which allows the development of strong hydrogen bridges. The NH stretching vibration is either downshifted to the region of the CH stretching vibrations as a result of the strong hydrogen bridging or it is broadened to such an extent that it is not seen in the experimental spectrum.

3.2. Raman Spectroscopy. The Raman spectrum is shown in Figure 3. Wavenumbers and relative intensities of the bands are collected in Table 2. The only signals that appear above 1700 cm^{-1} are the signals in the CH stretching region. Again, there is no detectable signal that can be related to a NH stretching vibration. A comparison of the IR and the Raman

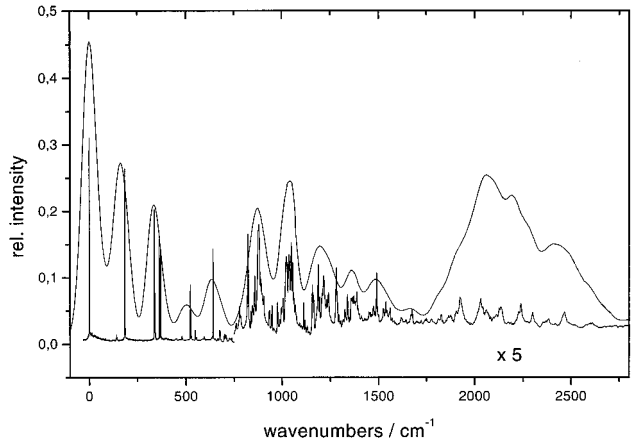

Figure 4. Matrix isolation UV spectrum and site-selective fluorescence excitation spectrum of porphycene.

TABLE 3: Location of the Maxima of Vibronic Bands in the Low-Energy (Q-Band) Region of the Porphycene Absorption Spectrum Observed under Different Experimental Conditions

	2-MTHF/$T = 77$ K $\tilde{\nu}$/cm^{-1}	Ar matrix/$T = 12$ K $\tilde{\nu}$/cm^{-1}	Solvens shift Δ/cm^{-1}
1	15913	16007	94
2	16080	16177	97
3	16252	16348	96
4		16510	
5	16543	16642	99
6	16756	16892	136
7	16909	17044	135
8	17097	17205	108
9		17370	
10	17422	17509	87
11	17899	18079	180
12	18109	18213	104
13	18325	18472	147

spectrum does not reveal bands that appear in both spectra. There is no indication for a breakdown of the exclusion principle. This is another strong argument for the existence of a center of symmetry.

3.3. Site-Selective Fluorescence and Fluorescence Excitation Spectroscopy. Standard UV and fluorescence spectra of porphycene are known from measurements in solution at room temperature and from measurements in organic glasses at liquid nitrogen temperature.[20] The general structure of the UV spectrum is the one known for all porphyrinoid systems. It consists of two weak bands at low energies, the so-called Q-bands (L-bands in the nomenclature of the polycyclic aromatic hydrocarbons (PAH)), and a strong band system around 30000 cm^{-1} which is called Soret band (B-bands in PAH). The Q-bands are related to transitions from the ground state to the first two excited singlet states. In less symmetric systems the Soret band is split into two bands or at least exhibits a pronounced shoulder.

Figure 4 shows the Q-band region of the absorption spectrum of **1** measured in an Ar matrix at 12 K together with the site-selective fluorescence excitation spectrum obtained from site (B). The 0−0 transition of this site is located at 15 971.4 cm^{-1}. The absorption spectrum consists of three band systems that cover the spectral regions 15900−16600 cm^{-1}, 16600−17600 cm^{-1}, and 17600−18600 cm^{-1}. The first two contain well-resolved vibronic bands with a half-width of less than 200 cm^{-1}. The position of the maxima of these bands are collected in Table 3 and compared to similar data from a measurement in 2-MTHF (2-methyltetrahydrofuran) glass.[20] All vibronic bands exhibit the expected high-energy shift when we go from the 2-MTHF glass to the argon matrix. The fact that the shift differs for the first and the second band system confirms the assumption that these two band systems result from different electronic transitions. This assumption was first derived from the magnetically induced circular dichroism (MCD) spectrum[20] that shows a change in the sign of the B-term at the onset of the second band system. The larger shift of the second system indicates a higher f value for the S_0-S_2 transition compared to that of S_0-S_1.

TABLE 4: Energies and Intensities of Bands Observed in the Fluorescence Excitation Spectrum of Porphycene[a]

$\tilde{\nu}$/cm^{-1}	int	ass.	$\tilde{\nu}$/cm^{-1}	int
142.4	54	1	1036.7	102
185.1	1000	2	1048.7	115
337.5	767	3	1056.3	93
362.8	596	4a	1069.7	45
369.5	542	4b	1112.2	47
449.0	32	2 * x ($x = 225$)	1119.0	27
479.5	45	1 + 3	1130.5	21
523.2	337	2 + 3	1157.3	67
548.2	81	2 + 4a	1188.4	91
554.0	38	2 + 4b	1215.4	77
595.3	43	x + 4b	1231.5	50
633.3	38		1240.2	58
640.5	543	6	1281.7	87
651.9	31		1324.7	39
663.9	32		1339.2	57
675.3	79	2 * 3	1357.6	52
699.7	57	3 + 4a	1371.2	55
706.7	54	3 + 4b	1386.4	59
724.6	33		1472.7	43
731.1	32		1490.2	81
737.8	37		1525.6	40
761.5	24		1538.2	48
778.2	43	1 + 6	1560.5	41
783.2	33		1675.1	39
822.6	126	2 + 6	1826.9	34
837.7	38		1906.1	37
846.5	44		1924.7	53
858.2	78		2031.5	52
879.7	136		2059.6	39
905.2	55		2133.9	42
933.0	37		2238.8	46
935.9	39		2299.7	36
948.0	44		2383.5	28
977.5	47	3 + 6	2465.9	36
1006.2	52		2613.5	24
1023.3	99			

[a] The energies refer to the 0−0 transition at 16 033.1 cm^{-1}. The intensities are relative to the intensity of the band at 185.1 cm^{-1} which was set to 1000.

The energies and relative intensities of all peaks that are clearly discernible in our fluorescence excitation (FE) spectrum (Figure 4) up to an excess energy of 2600 cm^{-1} are listed in Table 4. At an excess energy of about 850 cm^{-1} the spectrum starts to become highly congested. No similar congestion is observed in the fluorescence spectrum (Figure 5). The congestion in the absorption spectrum is another indication for the existence of two overlapping electronic bands where the vibronic states result from a complex interaction between two manifolds. To locate the 0−0 transition of S_2 it is necessary to study the shifts resulting from the use of different matrix materials or with respect to a jet spectrum. Such a study is beyond the scope of the present investigation.

The fluorescence (F) spectrum (Figure 5) shows some site contamination which is best seen with the 0−0 transition and the strong signals at 180.5 and 344.1 cm^{-1}. Peak positions and relative intensities are collected in Table 5. Up to an excess energy of 800 cm^{-1}, that is, in the region where the FE spectrum is not perturbed by overlapping electronic transitions, we find

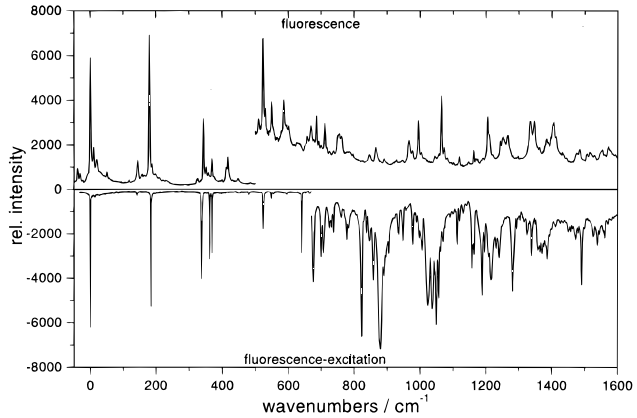

Figure 5. Site-selective fluorescence and fluorescence excitation spectrum of porphycene in argon matrix.

TABLE 5: Energies and Intensities of Bands Observed in the Fluorescence Spectrum of Porphycene[a]

$\tilde{\nu}$/cm^{-1}	int	ass.	$\tilde{\nu}$/cm^{-1}	int
145.6	188	1	965.8	32
158.1	99	2	995.5	44
180.5	1000	3	1064.7	61
221.4	59	4	1072.9	27
327.0	71	1 + 3	1118.7	21
344.1	458	5	1162.7	25
369.7	198	6	1205.0	48
412.4	143		1244.4	31
417.3	210		1251.6	34
446.9	70	2 * 4	1266.7	35
490.0	1	1 + 5	1333.4	44
523.2	9813	3 + 5	1347.4	44
549.6	5765	3 + 6	1384.3	33
585.9	67	4 + 6	1406.3	43
669.0	41	7	1484.8	26
686.1	48	2 * 5	1506.8	23
711.7	43	5 + 6	1515.6	24
755.6	37		1529.4	23
761.3	35		1552.7	26
846.5	23		1571.9	28
865.9	27		1618.0	31
891.3	20			

[a] The energies refer to the 0−0 transition at 15 969.6 cm^{-1}. The intensities are relative to the intensity of the band at 180.5 cm^{-1} which was set to 1000.

the expected similarity between fluorescence and fluorescence excitation spectrum. There are only three clearly detectable deviations from mirror symmetry in this energy range: The band at 370 cm^{-1} in F corresponds to a double band at 363 and 370 cm^{-1} in FE, the doublet at 412 and 417 cm^{-1} in F has no counterpart in FE, and the intense band at 641 cm^{-1} in FE is not observed in F. However, the latter band has a clearly discernible counterpart in the low-resolution absorption spectrum which shows the same solvent shift as the 0−0 transition of S_1. For this reason we assign the band at 641 cm^{-1} to a vibronic band of S_1. This assignment is further confirmed by the observation of fairly strong combinations with the 142, the 185, and the 337 cm^{-1} modes. Furthermore, the combination bands at 822.6 cm^{-1} and at 977.5 cm^{-1} in FE are among the few sharp bands at excess energies of more than 800 cm^{-1}, another hint for its affiliation with the S_1 state.

The bands marked with an one digit number in Table 5 coincide within a few wavenumbers with bands that also appear in the Raman spectrum. All other bands below 700 cm^{-1} (with the exception of the double band at 412/417 cm^{-1}) can be assigned to combinations. None of the bands that appear in this energy region correspond to any band observed in the IR spectra. This and the correspondence with the Raman spectrum provide considerable evidence that the marked bands relate to ground-state fundamentals.

TABLE 6: Calculated Frequencies and IR Intensities of the Normal Modes of *trans*-Porphycene

ass.	$\tilde{\nu}$/cm^{-1}	ass.	$\tilde{\nu}$/cm^{-1}	ass.	$\tilde{\nu}$/cm^{-1}	int	ass.	$\tilde{\nu}$/cm^{-1}	int
$1a_g$	150.4	$1b_g$	117.1	$1a_u$	60.4		$1b_u$	236.5	1.7
$2a_g$	202.8	$2b_g$	150.9	$2a_u$	71.6	1.7	$2b_u$	325.4	2.8
$3a_g$	341.4	$3b_g$	196.3	$3a_u$	85.0	7.7	$3b_u$	383.7	9.7
$4a_g$	357.7	$4b_g$	206.1	$4a_u$	215.6	0.7	$4b_u$	461.7	13.2
$5a_g$	478.9	$5b_g$	395.8	$5a_u$	306.2	2.4	$5b_u$	609.2	1.7
$6a_g$	594.4	$6b_g$	491.4	$6a_u$	318.2	0.9	$6b_u$	663.5	9.9
$7a_g$	660.2	$7b_g$	640.4	$7a_u$	511.9		$7b_u$	828.5	6.4
$8a_g$	817.7	$8b_g$	657.6	$8a_u$	629.6	0.7	$8b_u$	886.7	40.8
$9a_g$	866.5	$9b_g$	703.6	$9a_u$	664.6	27.7	$9b_u$	895.2	72.5
$10a_g$	937.9	$10b_g$	714.3	$10a_u$	711.6	0.4	$10b_u$	919.8	155.9
$11a_g$	951.6	$11b_g$	772.7	$11a_u$	716.2	0.2	$11b_u$	970.4	0.4
$12a_g$	959.0	$12b_g$	783.5	$12a_u$	750.5	55.2	$12b_u$	1054.8	33.9
$13a_g$	1068.8	$13b_g$	821.1	$13a_u$	806.0	7.1	$13b_u$	1080.1	78.1
$14a_g$	1083.7	$14b_g$	879.2	$14a_u$	820.6	144.9	$14b_u$	1087.7	81.4
$15a_g$	1100.5	$15b_g$	886.4	$15a_u$	878.4	0.3	$15b_u$	1129.6	40.6
$16a_g$	1132.8	$16b_g$	943.4	$16a_u$	887.4	2.0	$16b_u$	1182.6	3.9
$17a_g$	1174.1	$17b_g$	1103.2	$17a_u$	943.1		$17b_u$	1185.8	18.8
$18a_g$	1200.2			$18a_u$	1162.2	140.8	$18b_u$	1204.2	35.1
$19a_g$	1212.4						$19b_u$	1248.8	101.4
$20a_g$	1278.6						$20b_u$	1288.9	6.4
$21a_g$	1317.0						$21b_u$	1340.8	23.4
$22a_g$	1337.0						$22b_u$	1372.8	14.4
$23a_g$	1384.4						$23b_u$	1392.7	0.6
$24a_g$	1389.9						$24b_u$	1430.5	110.4
$25a_g$	1421.8						$25b_u$	1441.8	51.6
$26a_g$	1465.5						$26b_u$	1490.3	22.1
$27a_g$	1497.1						$27b_u$	1493.5	29.6
$28a_g$	1522.3						$28b_u$	1554.2	57.3
$29a_g$	1543.5						$29b_u$	1586.3	133.5
$30a_g$	1612.8						$30b_u$	2529.4	522.8
$31a_g$	2522.3						$31b_u$	3068.3	8.6
$32a_g$	3068.4						$32b_u$	3087.4	45.5
$33a_g$	3087.6						$33b_u$	3158.1	7.0
$34a_g$	3158.2						$34b_u$	3171.2	2.8
$35a_g$	3171.3						$35b_u$	3181.6	30.9
$36a_g$	3181.7						$36b_u$	3192.4	21.5
$37a_g$	3192.6								

In the excitation spectrum we did not observe any signals that correspond to the weak bands at 158 and 221 cm^{-1} in the fluorescence spectrum. However, a band at 449 cm^{-1} can be interpreted as the overtone of a 225 cm^{-1} vibration because of the appearance of the comparable overtone in F. The splitting of the band around 366 cm^{-1} in the FE spectrum is most likely caused by Fermi resonance with the first overtone of the mode at 185 cm^{-1}. The vibrations that are considered to represent fundamentals of S_1 are marked with one digit numbers in Table 4. The differences between S_0 and S_1 fundamentals are very small except for the mode around 650 cm^{-1}. This is the same mode that shows a totally different intensity in F and FE.

4. Comparison with Calculations

Calculated harmonic frequencies and IR intensities are collected in Tables 6 and 7 for *trans*- and *cis*-porphycene, respectively. All frequencies have been scaled by 0.995, the factor recomended by Pulay for DFT calculations that involve BLYP potentials.[38] Both results are compared in Figure 6 to the IR spectrum that we obtained from the KBr pellet. The two calculated spectra are surprisingly similar—despite the lack of a center of symmetry in the cis form. Most of the transitions that become symmetry-allowed going from the trans to the cis form do not gain a great deal of intensity. The behavior of the skeleton seems to depend very little on the actual location of the inner protons. Therefore, the number of bands that we expect to see in an experimental spectrum does not increase for the cis form. The spectrum is determined primarily by a D_{2h} pseudosymmetry.

TABLE 7: Calculated Frequencies and IR Intensities of the Normal Modes of *cis*-Porphycene

ass.	$\tilde{\nu}$/cm^{-1}	int	ass.	$\tilde{\nu}$/cm^{-1}	int	ass.	$\tilde{\nu}$/cm^{-1}	ass.	$\tilde{\nu}$/cm^{-1}	int
$1a_1$	217.6	2.0	$1b_1$	70.9	1.7	$1a_2$	60.2	$1b_2$	145.3	
$2a_1$	240.2	2.9	$2b_1$	84.7	7.9	$2a_2$	115.7	$2b_2$	325.3	1.9
$3a_1$	341.2	0.3	$3b_1$	154.8	0.2	$3a_2$	203.0	$3b_2$	459.3	11.0
$4a_1$	356.6		$4b_1$	197.3	0.1	$4a_2$	215.1	$4b_2$	478.5	
$5a_1$	386.7	9.8	$5b_1$	306.4	3.1	$5a_2$	316.7	$5b_2$	591.4	0.4
$6a_1$	607.3	0.9	$6b_1$	490.8		$6a_2$	395.2	$6b_2$	660.9	8.7
$7a_1$	661.8	0.1	$7b_1$	629.3	1.0	$7a_2$	511.3	$7b_2$	807.5	0.3
$8a_1$	824.8	5.7	$8b_1$	641.1	0.1	$8a_2$	656.0	$8b_2$	858.8	1.1
$9a_1$	874.3	51.8	$9b_1$	664.3	26.3	$9a_2$	702.6	$9b_2$	894.4	0.2
$10a_1$	942.6	5.1	$10b_1$	713.9	0.2	$10a_2$	713.2	$10b_2$	921.5	132.9
$11a_1$	957.0	46.0	$11b_1$	750.6	46.5	$11a_2$	718.1	$11b_2$	945.4	1.4
$12a_1$	978.4	4.3	$12b_1$	784.7	0.1	$12a_2$	772.8	$12b_2$	1053.8	22.4
$13a_1$	1076.8	96.5	$13b_1$	817.0	161.4	$13a_2$	808.2	$13b_2$	1069.2	0.3
$14a_1$	1084.5	21.8	$14b_1$	882.5	0.3	$14a_2$	818.8	$14b_2$	1084.1	33.9
$15a_1$	1105.6	0.9	$15b_1$	888.4	2.0	$15a_2$	881.2	$15b_2$	1112.0	0.3
$16a_1$	1162.5	14.2	$16b_1$	939.5		$16a_2$	886.6	$16b_2$	1166.9	20.6
$17a_1$	1175.6	7.1	$17b_1$	1207.5	138.4	$17a_2$	939.2	$17b_2$	1184.9	9.6
$18a_1$	1198.5	3.1				$18a_2$	1145.6	$18b_2$	1211.7	16.7
$19a_1$	1223.8	128.1						$19b_2$	1229.7	44.9
$20a_1$	1283.9	10.1						$20b_2$	1282.8	7.1
$21a_1$	1327.6	1.0						$21b_2$	1324.9	3.3
$22a_1$	1371.9	15.1						$22b_2$	1342.5	4.7
$23a_1$	1385.0	0.4						$23b_2$	1384.0	6.9
$24a_1$	1419.3	41.3						$24b_2$	1392.5	1.6
$25a_1$	1444.8	6.7						$25b_2$	1433.3	119.8
$26a_1$	1490.5	47.8						$26b_2$	1463.9	17.7
$27a_1$	1501.6	35.2						$27b_2$	1492.6	8.1
$28a_1$	1539.7	0.1						$28b_2$	1516.1	17.0
$29a_1$	1553.9	67.4						$29b_2$	1570.7	26.4
$30a_1$	1617.5	120.3						$30b_2$	2227.2	6.0
$31a_1$	2271.7	527.2						$31b_2$	3070.5	0.8
$32a_1$	3070.5	5.8						$32b_2$	3088.5	46.9
$33a_1$	3088.6							$33b_2$	3157.5	6.2
$34a_1$	3159.2	0.5						$34b_2$	3170.1	2.4
$35a_1$	3172.2	0.1						$35b_2$	3180.6	8.6
$36a_1$	3184.2	26.3						$36b_2$	3189.7	5.1
$37a_1$	3192.8	13.5								

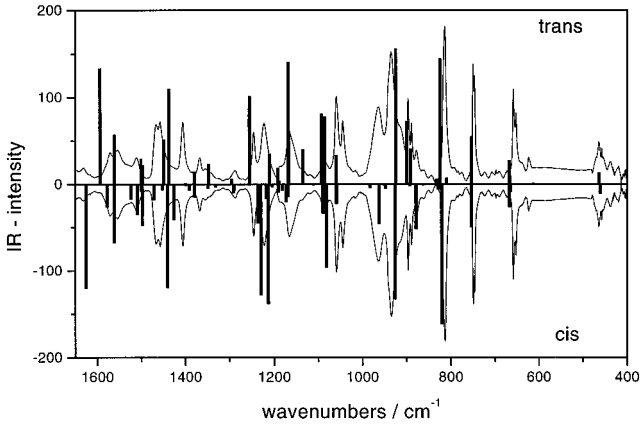

Figure 6. Calculated IR spectrum of *cis*- and *trans*-porphycene in comparison to the experimental IR spectrum.

Comparison between theory and experiment does not permit us to decide between the cis and the trans form. There is a slightly better coincidence with the theoretical trans spectrum but the average deviation between theory and experiment is similar to the deviation between the two calculations. We did not actually calculate Raman intensities. However, the fact that the IR intensities of the transitions that violate the mutual exclusion principle in *cis*-porphycene are all predicted to be very low makes us wonder if the same is not true for the Raman intensities. Therefore, the fact that we do not observe a major violation of the exclusion principle in the experimental spectra is, in our opinion, no proof for the existence of a center of symmetry.

Further comparison of predicted and observed spectra reveals a puzzling result: For both forms the calculations predict very intense bands around 2500 cm^{-1} that relate to NH stretching vibrations. The low energy of this special vibration is probably due to difficulties all DFT methods seem to have with the description of the (N−H···N) hydrogen bridges in the cavity. The energy increases by about 200 cm^{-1} if the B3 exchange potential is applied instead of the B potential.[14] Comparable RHF calculations predict 3025 cm^{-1} for the trans and 3062 cm^{-1} for the cis form (after scaling with a factor of 0.89 as recommended by Pulay[38] for HF calculations), which is much closer to what one would expect by comparison to **2**. The increase in wavenumber parallels a decrease in (NH) bond length that is grossly overestimated in BLYP calculations. However, all calculations including RHF predict the NH stretching vibration to be the most intense vibration in the entire spectrum, about twice as intense as all the other ones. No indication of such an intense transition is found in the experimental IR spectra. There are only two possibilities for the resolution of this puzzle: Either all theoretical methods overestimate the intensity by at least a factor of 10, which is very unlikely, or the band is strongly broadened because of the rapid motion of the proton in the hydrogen bridge and therefore disappears in the background.

Before we compare the theoretical results with the vibrations observed in the electronic spectra we must discuss which vibrations we anticipate to find. All (π,π*)-excited electronic states of the planar trans form that can be reached from the ground state by an allowed one-photon transition belong to the irreducible representation (irrep) B_u. Only g vibrations can be

TABLE 8: Comparison of Experimental and Theoretical Results for Vibronically Active Modes

experiment				calculation			
fluorescence		Raman		trans		cis	
$\tilde{\nu}$/cm^{-1}	int	$\tilde{\nu}$/cm^{-1}	int	ass.	$\tilde{\nu}$/cm^{-1}	ass.	$\tilde{\nu}$/cm^{-1}
146	188	141	23	$1a_g$	150	$1b_2$	145
158	99	159	28	$2b_g$	151	$3b_1$	155
				$3b_g$	196	$4b_1$	197
181	1000	182	30	$2a_g$	203	$1a_1$	218
221	59	222	29	$4b_g$	206	$3a_2$	203
344	458	344	65	$3a_g$	341	$3a_1$	341
370	198	367	46	$4a_g$	358	$4a_1$	357
		400	12	$5b_g$	396	$6a_2$	395
		479	6	$5a_g$	479	$4b_2$	479
				$6b_g$	491	$6b_1$	491
		597	12	$6a_g$	594	$5b_2$	591
		650	8	$7b_g$	640	$8b_1$	641
				$8b_g$	658	$8a_2$	656
669	41	666	19	$7a_g$	660	$7a_1$	662
		701	17	$9b_g$	704	$9a_2$	703

excited together with the electronic state. The a_g vibrations can couple either directly via the Condon term or indirectly through first-order Herzberg Teller coupling. This situation can lead to interferences that cause deviations from the mirror image symmetry between absorption and fluorescence.[39,40] The b_g modes can contribute only through coupling to out-of-plane polarized (σ,π^*)-type transitions which are always weak. Therefore, if they appear at all, b_g modes should appear with very low intensity.

The one-photon allowed (π,π^*)-transitions of the planar cis form belong to irrep A_1 or to irrep B_2. The a_1 modes can gain intensity directly or indirectly by vibronic coupling. The b_2 modes can introduce vibronic coupling between A_1 and B_2 states and vice versa. The a_2 and b_1 modes can only appear through coupling with out-of-plane polarized transitions.

The data shown in Table 8 yield a comparison of calculated and observed vibrations in the energy range up to 700 cm^{-1}. The a_g and b_g modes for the trans form are listed as well as the vibrations that resemble these modes most closely in the cis form. The correlation between trans and cis is straightforward with the exception of $4b_g$ which relates to $3a_2$ and $4a_2$. The calculated frequencies are very similar for the two forms of **1**, a fact we already observed for the IR active modes.

The modes that lead to intense vibronic bands in the fluorescence spectrum are easily assigned to the first four a_g modes in the case of the trans form or, equally well, to the in-plane modes $1b_2$, $1a_1$, $3a_1$, and $4a_1$, in the case of the cis form. The mode that is observed at 666 cm^{-1} in the Raman spectrum and with very low intensity at 669 cm^{-1} in the fluorescence spectrum corresponds equally well to $7a_g$ or $7a_1$. There are no in-plane vibrations that fit the bands at 158 and 221 cm^{-1}. These bands must result from out-of-plane vibrations ($2b_g$ and $4b_g$ in the trans form and $3b_1$ and $3a_2$ in the cis form); this is in agreement with the very low intensity of these bands. The five weak signals that appear in the Raman spectrum between 400 and 700 cm^{-1} are again equally well assigned to calculated frequencies of both forms (Table 8). The signals at 400, 650, and 701 cm^{-1} are related to the out-of-plane modes $5b_g$, $7b_g$, and $9b_g$ or $6a_2$, $8b_1$, and $9a_2$, respectively. The signals at 479 and 597 cm^{-1} can be assigned to the in-plane modes $5a_g$ and $6a_g$ of the trans form or to $4b_2$ and $5b_2$ in the case of the cis structure.

Similar to the IR spectrum, the analysis of the high-resolution fluorescence spectrum does not distinguish with certainty between *trans*- and *cis*-porphycene. The better agreement of $2a_g$ with the band at 180 cm^{-1} compared to $1a_1$ favors the trans form but is not convincing. The only major difference between the trans and cis forms found among the theoretical results concerns the medium intense band at 146 cm^{-1}. In the trans form this band is Condon-allowed whereas in the cis form it results only from vibronic coupling. If porphycene exists in the cis form, the band at 146 cm^{-1} has to be polarized perpendicular to the 0−0 transition and to the band at 180 cm^{-1} excess energy. Further investigations should determine if measurements with polarized light can make use of this prediction.

Conclusions

Porphycene turns out to be a case where vibrational spectroscopy, like all other experimental information available until now, is not able to provide a definitive proof that it exists in the trans form as predicted by more advanced theoretical calculations. The loss of the center of inversion in going from trans to cis causes only minor changes in calculated frequencies and intensities, changes much too subtle for a comparison with experimental data. The nearly perfect obedience of the exclusion principle in IR and Raman spectra and the agreement between vibronic fluorescence and Raman bands are no sufficient proof for the trans form. The data calculated for the cis form explain the experimental findings nearly equally well. The reason is that the geometric and electronic structure of the macrocyclic ring is hardly influenced at all by the positions of the hydrogen atoms in the inner cavity. Whether this is a general characteristic of porphyrinoids that is caused by a kind of supersymmetry of the carbon nitrogen skeleton or a special property of porphycene that results from the strong hydrogen bridges is a question that is part of our ongoing work.

Acknowledgment. We want to thank Prof. H. W. Siesler, Universitaet Gesamthochschule Essen, for the recording of the Raman spectrum and Prof. Dr. E. Vogel and Dipl. Chem. F. Zuniga y Rivero for supplying us with porphycene. Further we wish to thank the Regionales Rechenzentrum der Universitaet zu Koeln for providing the computational resources.

References and Notes

(1) Vogel, E.; Koecher, M.; Schmickler, H.; Lex, J. *Angew. Chem.* **1986**, *98*, 262.
(2) Battersby, A. R.; Fookes, C. J. R.; Matcham, G.-W. J.; McDonald, E. *Nature* **1980**, *285*, 17.
(3) Sessler, J. L.; Brucker, E. A.; Weghorn, S. J.; Kisters, M.; Schaefer, M.; Lex, J.; Vogel, E. *Angew. Chem.* **1994**, *106*, 2402.
(4) Callot, H. J.; Rohrer, A.; Tschamber, T.; Metz, B. *New J. Chem.* **1995**, *19*, 155.
(5) Vogel, E.; Broering, M.; Weghorn, S. J.; Scholz, P.; Deponte, R.; Lex, J.; Schmickler, H.; Schaffner, K.; Braslavsky, S. E.; Mueller, M.; Poerting, S.; Fowler, C.; Sessler, J. L. *Angew. Chem.*, submitted.
(6) Franck, B.; Nonn, A. *Angew. Chem.* **1995**, *107*, 1941.
(7) Zerbetto, F.; Zgierski, M. Z.; Orlandi, G. *Chem. Phys. Lett.* **1987**, *139*, 401.
(8) Almloef, J.; Fischer, T. H.; Gassman, P. G.; Ghosh, A.; Haeser, M. *J. Phys. Chem.* **1993**, *97*, 10964.
(9) Reynolds, C. H. *J. Org. Chem.* **1988**, *53*, 6061.
(10) Lamoen, D.; Parrinello, M. *Chem. Phys. Lett.* **1996**, *248*, 309.
(11) Merchan, M.; Orti, E.; Roos, B. *Chem Phys. Lett.*. **1994**, *221*, 136.
(12) Hohlneicher, G.; Karuth, V.; Malsch, K.; Roeb, M. In *Proceedings of the 10th International Symposium on Atomic, Molecular, Cluster, Ion, and Surface Physics*; 1996; p 159.
(13) Karuth, V.; Malsch, K.; Roeb, M.; Hohlneicher, G. *Chem. Phys.*, in press.
(14) Malsch, K. Master's thesis, Koeln, 1996.
(15) Almloef, J.; Ghosh, A. *J. Phys. Chem.* **1995**, *99*, 1073.
(16) Reimers, J. R.; Lue, T. X.; Crossley, M. J.; Hush, N. S. *J. Am. Chem. Soc.* **1995**, *117*, 2855.
(17) Wehrle, B.; Limbach, H.-H.; Koecher, M.; Ermer, O.; Vogel, E. *Angew. Chem.* **1987**, *99*, 914.
(18) Schlabach, M.; Rumpel, H.; Limbach, H.-H. *Angew. Chem.* **1989**, *101*, 84.

(19) Braun, J.; Schlabach, M.; Wehrle, B.; Koecher, M.; Limbach, H.-H.; Vogel, E. *J. Am. Chem. Soc.* **1994**, *116*, 6593.

(20) Waluk, J.; Mueller, M.; Swiderek, P.; Koecher, M.; Vogel, E.; Hohlneicher, G.; Michl, J. *J. Am. Chem. Soc.* **1991**, *113*, 5511.

(21) Radziszewski, J. G.; Waluk, J.; Nepras, M.; Michl, J. *J. Phys. Chem.* **1991**, *95*, 1963.

(22) Radziszewski, J. G.; Waluk, J.; Michl, J. *J. Mol. Spectrosc.* **1990**, *140*, 373.

(23) Radziszewski, J. G.; Waluk, J.; Michl, J. *Chem. Phys.* **1989**, *136*, 165.

(24) Radziszewski, J. G.; Nepras, M.; Balaji, V.; Waluk, J.; Vogel, E.; Michl, J. *J. Phys. Chem.* **1995**, *99*, 14254.

(25) Voelker, S.; Macfarlane, R. M.; Genack, A. Z.; Trommsdorff, H. P.; van der Waals, J. H. *J. Chem. Phys.* **1977**, *67*, 1759.

(26) Even, U.; Jortner, J. *J. Chem. Phys.* **1982**, *77*, 4391.

(27) Waluk, J.; Vogel, E. *J. Phys. Chem.* **1994**, *98*, 4530.

(28) Kozlowski, P. M.; Zgierski, M. Z.; Pulay, P. *Chem. Phys. Lett.* **1995**, *247*, 379.

(29) Kozlowski, P. M.; Jarzecki, A. A.; Pulay, P. *J. Phys. Chem.* **1996**, *100*, 7007.

(30) Kozlowski, P. M.; Jarzecki, A. A.; Pulay, P.; Li, X.-Y.; Zgierski, M. Z. *J. Phys. Chem.* **1996**, *100*, 13985.

(31) Roeb, M. Ph.D. Thesis, Koeln, 1996.

(32) Limbach, H.-H. Personal communication.

(33) Gutmann, M.; Baum, H. G.; Gonska, H.; Schoenzart, H.-F.; Hohlneicher, G. *Chem. Phys.* **1990**, *140*, 99.

(34) Keith, T. A.; Petersson, G. A.; Montgomery, J. A.; Raghavachari, K.; Al-Laham, M. A.; Zakrzewski, V. G.; Ortiz, J. V.; Foresman, J. B.; Cioslowski, J.; Stefanov, B. B.; Nanayakkara, A.; Challacombe, M.; Peng, C. Y.; Ayala, P. Y.; Chen, W.; Wong, M. W.; Andres, J. L.; Replogle, E. S.; Gomperts, R.; Martin, R. L.; Fox, D. J.; Binkley, J. S.; Defrees, D. J.; Baker, J.; Stewart, J. P.; Head-Gordon, M.; Gonzalez, C.; Pople, J. A. *Gaussian 94*, Tech. rep., Gaussian Inc.: Pittsburgh, PA, 1995.

(35) Becke, A. D. *Phys. Rev. A* **1988**, *38*, 3098.

(36) Lee, C.; Yang, W.; Parr, R. G. *Phys. Rev. B* **1988**, *37*, 785.

(37) Mason, S. F. *J. Chem. Soc.* **1958**, 976.

(38) Rauhut, G.; Pulay, P. *J. Phys. Chem.* **1995**, *99*, 3093.

(39) Hohlneicher, G.; Wolf, J. *Ber. Bunsen-Ges. Phys. Chem.* **1995**, *99*, 366.

(40) Geigle, K. P.; Wolf, J.; Hohlneicher, G. *J. Photochem. Photobiol., A: Chem.* **1997**, *105*, 183.